Wide-Band Superconductive Chirp Filters

MARK S. DiIORIO, RICHARD S. WITHERS, MEMBER, IEEE, AND ALFREDO C. ANDERSON

Abstract — **Chirp filters are described that consist of miniature tapped superconductive stripline. The stripline consists of 40-μm-wide niobium thin films in a spiral pattern on 125-μm-thick silicon wafers, and tapping is effected by backward-wave couplers between neighboring lines. Sophisticated fabrication and packaging techniques have led to a now mature technology. Devices with 2.6 GHz bandwidth and time–bandwidth products of 98 are routinely fabricated that exhibit amplitude errors within a few tenths of a decibel and phase errors within a fraction of a degree of theoretical. In pulse-compression tests, matched amplitude-weighted devices yield peak relative side-lobe levels of −32 dB.**

I. INTRODUCTION

A CHIRP FILTER is characterized by an impulse response which has an instantaneous frequency which increases or decreases linearly in time, and consequently has a linear group-delay versus frequency characteristic. As such they can be employed as matched filters for analog signal processing applications, such as high-performance radar [1], spread-spectrum communications [2], [3], and spectral analysis [4], [5].

Surface-acoustic-wave and acoustooptic technologies have produced useful devices with bandwidths as large as 1 GHz [6], [7]. More recently, superconductive technology has been employed to produce chirp filters with bandwidths as large as 2.6 GHz [8], [9]. This technology provides the three essential functions needed to produce the chirp filter: delaying the input signal, tapping the signal stream at specified delays and with specified weighting, and summing the tapped signals.

The basic concept is to utilize coupled miniature superconductive striplines on a low-loss dielectric to provide useful delay at microwave frequencies. The stripline itself has negligible dispersion since it is a superconducting TEM structure; the dispersion is built into the device by tapping the input stripline with backward-wave couplers [10]. The coupled signals are summed into the traveling wave along the output stripline. Use of electromagnetic delay lines offers wide bandwidth (potentially tens of GHz), although the large propagation velocity limits the delays to about 10 ns per meter. A long miniaturized stripline is thus required to achieve reasonable delay in a small package. Superconductors are necessary to avoid the large transmission loss which would otherwise result from fabrication of long (4 m), narrow (40 μm) striplines from normal metals.

Key figures of merit for the chirp filters are the bandwidth, B, and the delay or dispersion time, T. The time–bandwidth product, TB, is a measure of the signal-processing gain available from a matched pair of devices. Other important considerations concern the amplitude and phase deviations from ideal behavior. For matched-filter applications, such deviations are manifested by degraded side-lobe performance in pulse-compression tests [11]. Suppression of these side lobes, in any technology, requires amplitude-weighting the filters as well as retaining tight control over their amplitude- and phase-versus-frequency characteristics. In the past, nonidealities have substantially limited the side-lobe performance for superconductive chirp filters [9], [12].

In this paper we present high-performance superconductive chirp filters which operate over bandwidths of 2.6 GHz and larger. Previously, superconductive chirp filters were fabricated that, while demonstrating proof of principle, fell well short of theoretical expectations. Improvements to the fabrication and packaging technology have produced new devices that closely match the theoretical design and hence exhibit excellent compressed-pulse performance. Consequently, the superconductive chirp filter has matured to where it is now practical for a variety of analog signal processing applications. A complete description of the state of the art of this technology is presented here for the first time.

II. DEVICE STRUCTURE AND FABRICATION

The chirp filters consist of a coupled pair of superconductive striplines which are wound in a spiral fashion. The two striplines are coupled by a cascaded array of backward-wave couplers as shown in the schematic of Fig. 1. An input signal is launched as a forward-propagating wave on one of the lines. At specified points along the line pair, a fraction of the signal energy is coupled onto a backward-propagating wave on the second line. Each coupler has a peak response at frequencies for which the coupler length is equal to an odd number of quarter wavelengths. To obtain the desired chirped frequency-versus-delay characteristic, the reciprocal of the length of each coupler is made a linear function of the length along the line. The resulting structure then has a local resonant frequency that is a linear function of the delay. In Fig. 1 the coupler length gets longer to the right in the figure;

Manuscript received January 14, 1988; revised July 7, 1988. This work was supported by the Department of the Navy and the Air Force.

M. S. DiIorio was with the Lincoln Laboratory, Massachusetts Institute of Technology, Cambridge, MA. He is now with Biomagnetic Technologies, Inc., 4174 Sorrento Valley Blvd., San Diego, CA 92121

R. S. Withers and A. C. Anderson are with the Lincoln Laboratory, Massachusetts Institute of Technology, Cambridge, MA 02173-4708.

IEEE Log Number 8826038.

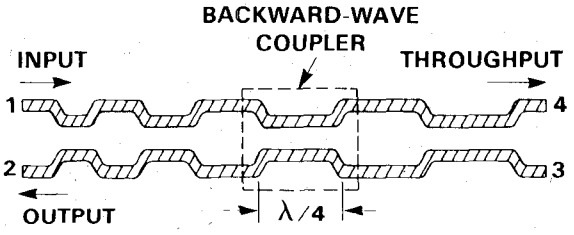

Fig. 1. Schematic of a chirp filter consisting of cascaded backward-wave couplers between neighboring striplines. A typical device comprises a few hundred couplers. Phase response is controlled by the length of the couplers, and amplitude response is controlled by the line-to-line separation.

consequently, lower frequencies suffer longer delays. The strength of each coupler can be controlled by varying the line spacing to give a desired amplitude weighting to the filter response. Also note that the chirp filter is a four-port device and can be used to produce either an up-chirp or a down-chirp by utilizing the appropriate pair of ports.

The chirp filters are designed from first principles, using coupling of modes theory [8]. The center frequency, bandwidth, insertion loss at center frequency, and weighting function are specified, and a grating function (coupling versus spatial coordinate) is generated. The grating function includes a correction for amplitude distortions caused by strong coupling and consequent input-wave depletion. A straightforward electromagnetic analysis is then used to specify the line spacing function and a photomask is produced.

The chirp filter is fabricated by sputtering Nb films onto 2-in-diameter, 125-μm-thick silicon wafers and using microlithographic techniques to pattern the films. Fig. 2 shows the silicon wafer containing the patterned center conductor; the ground plane has been deposited on the other side of the wafer. The second silicon wafer (not shown in Fig. 2) contains but a single Nb ground plane. The stripline structure is obtained by holding the two wafers together with mechanical spring pressure.

Nb is currently utilized for the superconductor because it is a refractory material and hence is extremely rugged. In addition, its superconducting transition temperature, 9.2 K, is safely above our device operating temperature of 4.2 K. Other, higher-transition-temperature superconductors could be utilized if they possessed low RF loss and could be deposited uniformly across the 2-in silicon substrates. Silicon is chosen for the dielectric because of its low loss, its high dielectric constant (which yields longer delay for a given substrate area), and its processing compatibility with Nb. Note that stripline is used because of superior isolation and dispersion characteristics compared with microstrip or coplanar designs occupying an equal substrate area. More extensive details of the device structure and fabrication can be found elsewhere [9], [13].

The chirp filters are designed to have 37.5 ns of dispersion and a 2.6 GHz bandwidth (centered at 4 GHz), for a time–bandwidth product of 98. For pulse compression, two types of chirp filters are constructed. One filter has a flat 5 dB insertion loss across the design bandwidth, while the other filter is amplitude-weighted for a Hamming [1]

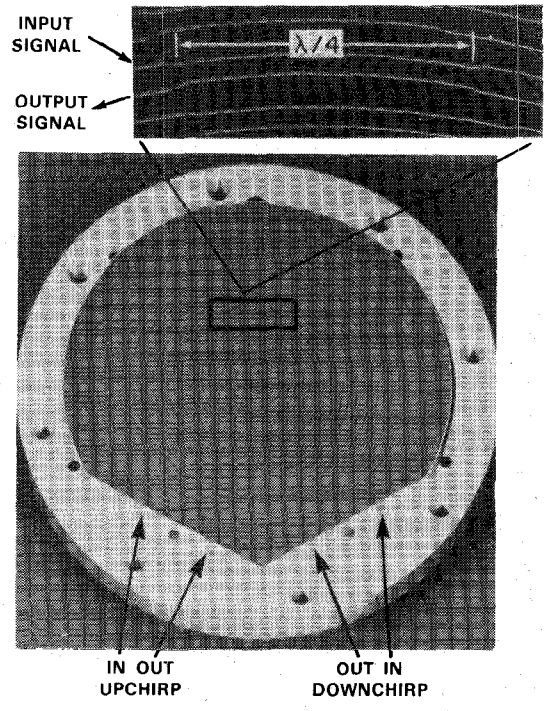

Fig. 2. Photograph of a quadruple-spiral coupled-stripline chirp filter. The 5-cm-diameter silicon substrate supports 3.3 m of 39-μm-wide niobium stripline. The upper silicon substrate (not shown) with its niobium ground plane is held in place by mechanical spring pressure. The inset shows a single coupler and neighboring lines.

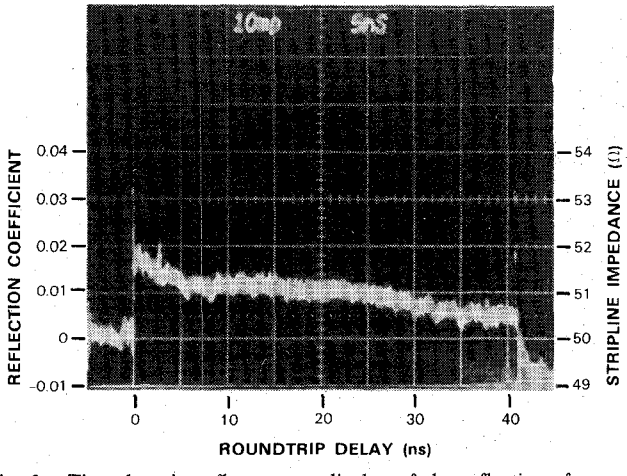

Fig. 3. Time-domain reflectometer display of the reflections from one of the two lines of a coupled-stripline chirp filter. The characteristic impedance is $51 \pm 0.5\ \Omega$ with rms deviations (neglecting the slow drift of the reflectometer baseline) of a few tenths of an ohm.

response with a 5 dB insertion loss at the center frequency. In the past, the chirp filters had been designed to have a 10-dB insertion loss. The stronger coupling in the present design is utilized to improve the ratio of desired to spurious signals in the device response, although this comes at the expense of limiting the theoretical side-lobe performance. The weaker coupling designs, however, were never able to reach their potentially superior side-lobe performance because of spurious signal reflections stemming from particulates lodging between the silicon substrates.

Careful packaging of the chirp filter is essential to obtain excellent device performance. The problems stem

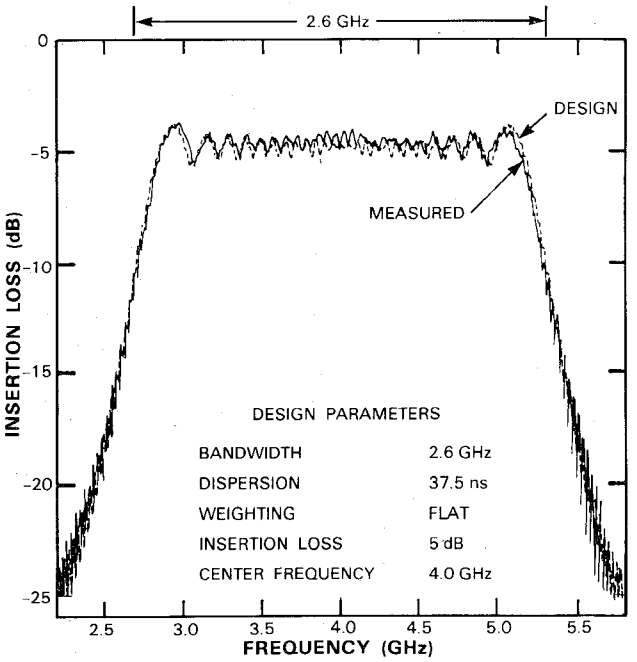

Fig. 4. Design-model and measured amplitude responses of a flat-weighted chirp filter.

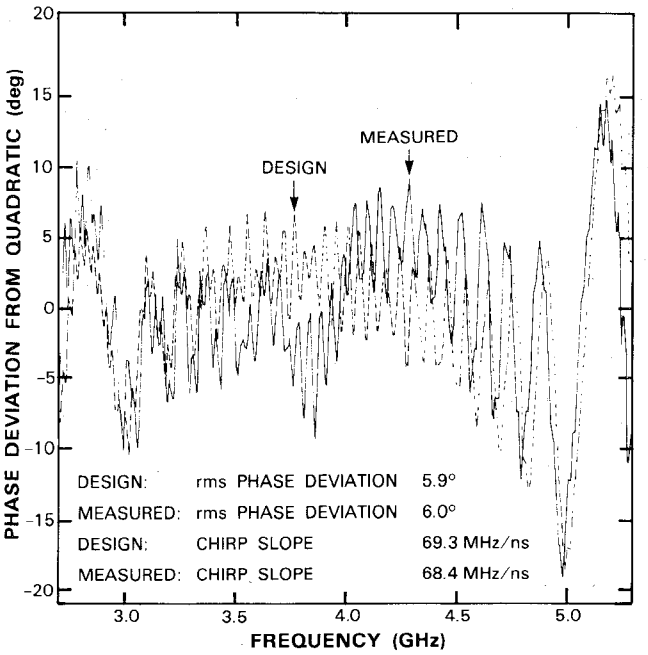

Fig. 5. Design-model and measured phase deviations of a flat-weighted chirp filter.

from the fact that the stripline is assembled from two separate thin substrates. Any particulates between the wafers can significantly alter the effective dielectric constant at those points, which changes the stripline impedance and produces spurious signal reflections. With sufficient attention toward maintaining clean wafers during fabrication and packaging, the yield of reproducible, high-performance devices readily exceeds 90 percent. The RF packages are also designed to prevent particulates from entering subsequent to the packaging process. Consequently, the devices can be subjected to repeated thermal cycling, from 300 K to 4.2 K and back, without degradation. Fig. 3 shows a time-domain reflectometry measurement for one of the chirp filters. The low level of spurious reflections (< 0.2 percent rms) indicates an absence of fabrication defects and particulates.

III. Results

The phase and amplitude responses of the chirp filters at 4.2 K were measured from 2 to 6 GHz using an HP 8408B automatic network analyzer. Both the measured and simulated amplitude responses of a flat-weighted device are shown together in Fig. 4. The simulations were made with the first-principles theory used to design the filter and were based on the physical design parameters of the device. Further details concerning the theory and simulations can be found elsewhere [8], [12]. The agreement between theory and experiment is excellent, even to the amplitude oscillations (Fresnel ripple), which are strongest at the frequency band edges. The Fresnel ripple stems from the discontinuity at the ends of the coupled lines; effectively the weighting function abruptly changes from zero to its constant design value (-5 dB here). The discontinuity in coupler strength also generates phase distortions which have the form of a decaying ripple. Fig. 5 shows the measured and simulated phase deviation from the best-fit quadratic. (Recall that since a chirp has a group delay that is linear in frequency, the phase is quadratic in frequency.) The measured best-fit quadratic yields a chirp slope that is within 1.3 percent of the designed chirp slope. The remaining phase error (deviation from quadratic) has a rms value of 6.0°, which is very close to the predicted rms phase error of 5.9°. Note further that the measured phase-deviation data closely track the simulated phase deviation, especially along the large-amplitude swings near the band edges, which are related to the Fresnel ripple.

The measured and simulated amplitude responses of a Hamming-weighted filter are shown in Fig. 6. Again the agreement is excellent. The phase deviation from quadratic is shown in Fig. 7. The measured chirp slope differs from the design value by 0.6 percent. The measured rms phase error has been weighted by the Hamming function to yield a weighted rms phase error of 3.1°, which compares favorably with the predicted weighted rms phase error of 3.5°. For comparison, the measured unweighted rms phase error is 4.7°, while the predicted unweighted error is 3.9°. The slowly varying sinusoidal shape of the phase deviation data stems from the strong coupling of the taps.

Note that the phase distortions caused by the strong tap weighting could be compensated by adjusting the tap weightings, i.e., by predistorting the device response [12]. Small imperfections in the device fabrication or packaging, most of which stem from small variations in the line width and submicron-size particulates between the wafers, can also effect such predistortions. These occasionally can even be beneficial, leading to a measured rms phase error that is less than the design, or simulated, rms phase error. Since the required predistortions are small, exceeding the design performance can only occur in devices which are carefully fabricated.

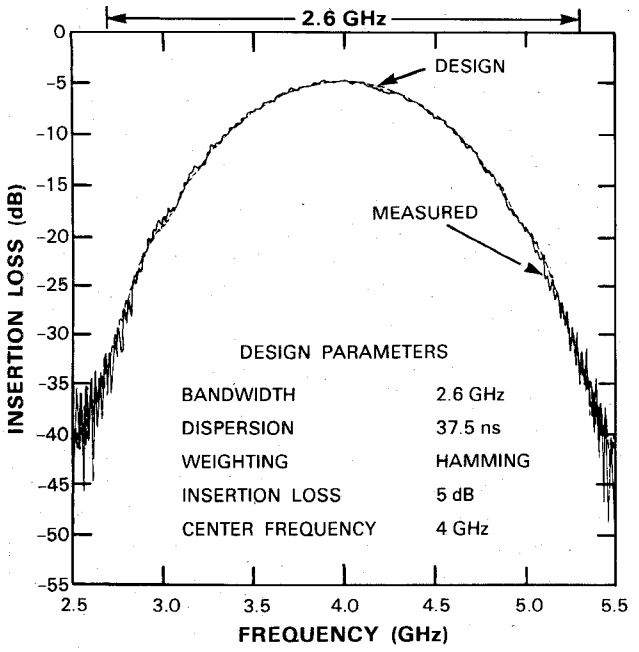

Fig. 6. Design-model and measured amplitude responses of a Hamming-weighted chirp filter.

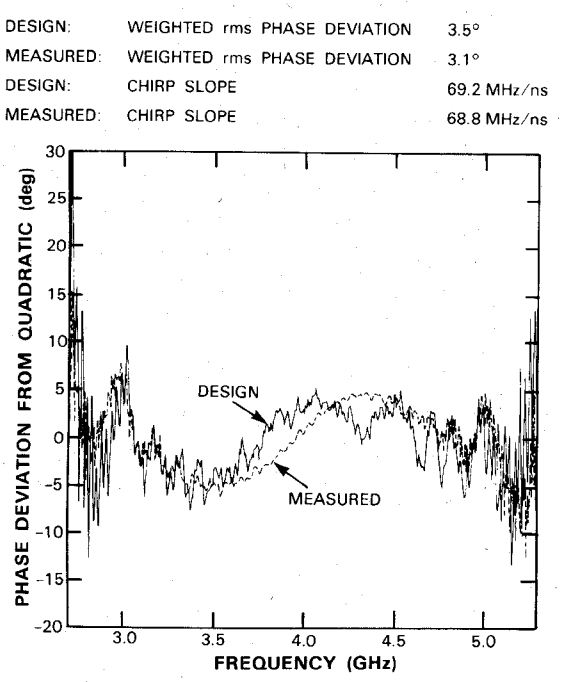

Fig. 7. Design-model and measured phase deviations of a Hamming-weighted chirp filter.

The compressed pulse response of a matched pair of chirp filters was obtained by applying a 7 V video impulse of 85 ps width to the input of a flat-weighted filter. The expanded up-chirp response was then directly applied to the down-chirp input port of the Hamming-weighted filter. Fig. 8 shows the resulting compressed pulse which has a 4 dB full width of 0.6 ns, consistent with the 2.6 GHz bandwidth and Hamming weighting (which broadens the compressed pulse). The largest side lobe lies at −32 dB relative to the central peak.

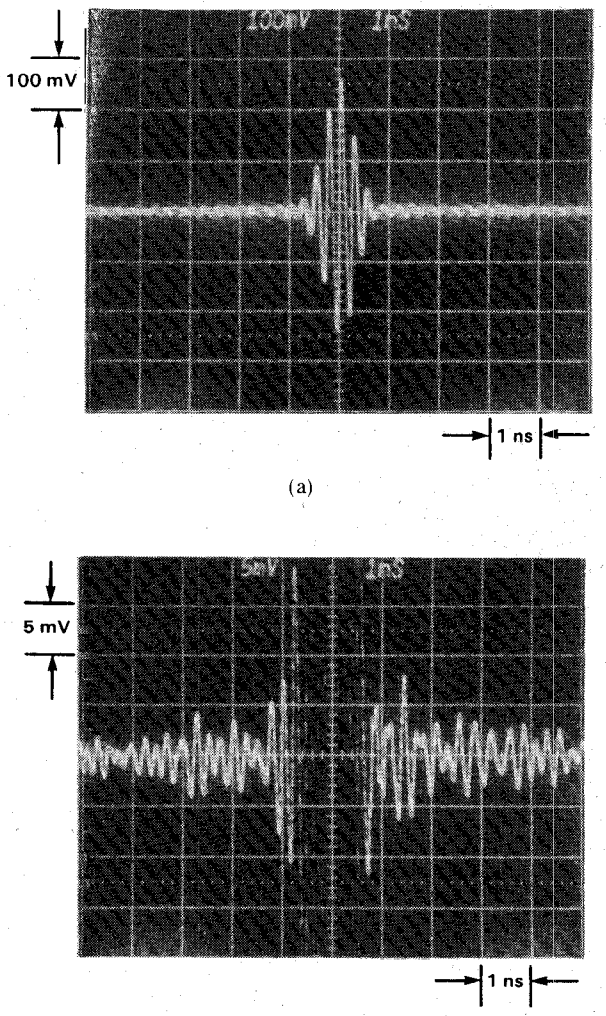

Fig. 8. (a) Compressed-pulse response of matched flat-weighted and Hamming-weighted chirp filters with 2.6 GHz bandwidth and 38-ns dispersion. (b) Compressed-pulse response displayed with 26 dB additional gain, demonstrating 32 dB peak relative side-lobe levels.

For comparison, the side-lobe level of the compressed-pulse response expected from the design is −30.5 dB. This is obtained by multiplying the transfer functions of the two filters (shown in Figs. 4 through 7) and then Fourier transforming to generate the compressed-pulse response. The 4 dB full width is 0.60 ns, which is in excellent agreement with the measured value. Note that to obtain the ideal −42 dB Hamming side lobes would require a design with a higher insertion loss (e.g., 20 dB) or, alternately, with phase predistortion [12] to compensate for the effects of strong tapping and the consequent input wave depletion. In the present case, small fabrication- and packaging-induced phase predistortions have caused the measured compressed-pulse response to exceed the low-insertion-loss design.

Wider bandwidth chirp filters have also recently been fabricated. These devices have a 6 GHz bandwidth (centered at 6 GHz), a delay time of 42 ns, and hence a time–bandwidth product of 252. The rms phase error for this flat-weighted device is 13.1° across the full 6 GHz bandwidth, even though the package is limiting the perfor-

mance at the higher frequencies. The rms phase error for the 3.5–6.0 GHz range is 5.6°.

One limitation of the present chirp filters is the relatively small delay. The amount of delay is limited by the length of stripline which can be fabricated on a wafer. The maximum length is primarily constrained by isolation requirements, which, in turn, are set by wafer (i.e., dielectric) thickness. Efforts are currently under way to increase the delay by (1) cascading the wafers and (2) developing thinner low-loss dielectric substrates [9].

IV. Conclusions

High-performance wide-band superconductive chirp filters have been demonstrated. Improvements to the fabrication and packaging processes have yielded excellent devices that closely match the design. The devices are rugged, reproducible, and thermally cyclable. Pulse compression with low relative side-lobe levels has been demonstrated over a 2.6 GHz bandwidth. The potential exists to increase both the bandwidth and the delay of these devices. Finally, note that development of low-loss, high-transition-temperature thin-film superconductors would allow operation of these devices in small closed-cycle cryocoolers.

Acknowledgment

The authors gratefully acknowledge the insightful efforts of P. G. Murphy and D. B. Whitley in the fabrication and packaging of these devices and the contributions of A. P. Denneno, J. Hamer, and W. P. Walker in mask layout, thin-film deposition, and device testing, respectively.

References

[1] C. E. Cook and M. Bernfeld, *Radar Signals*. New York: Academic, 1967.

[2] D. R. Arsenault, "Wideband chirp-transform adaptive filter," in *1985 Ultrasonics Symp. Proc.*, Oct 1985.

[3] J. H. Fischer, J. H. Cafarella, D. R. Arsenault, G. T. Flynn, and C. A. Bouman, "Wide-band packet radio technology," in *Proc. IEEE*, vol. 75, pp. 100–115, Jan. 1987.

[4] G. W. Judd and V. H. Estrick, "Applications of SAW chirp filters —An overview," *Proc. Soc. Photo-Opt. Instrum. Eng.*, vol. 239, pp. 220–235, 1980.

[5] R. S. Withers and S. A. Reible, "Superconductive chirp-transform spectrum analyzer," *IEEE Electron Device Lett.*, vol. EDL-6, pp. 261–263, June 1985.

[6] R. C. Williamson, "Properties and applications of reflective-array devices," *Proc. IEEE*, vol. 64, pp. 702–710, May 1976.

[7] L. C. Lennert, I. C. Chang, D. L. Steinmetz, W. Brooke, and F. Langdon, "High-performance GHz-bandwidth acoustooptic spectrum analyzer," in *Proc. Soc. Photo-Opt. Instrum. Eng.*, vol. 352, pp. 10–16, 1982.

[8] R. S. Withers, A. C. Anderson, P. V. Wright, and S. A. Reible, "Superconductive tapped delay lines for microwave analog signal processing," *IEEE Trans. Magn.*, vol. MAG-19, pp. 480–484, 1983.

[9] R. S. Withers, A. C. Anderson, J. B. Green, and S. A. Reible, "Superconductive delay-line technology and applications," *IEEE Trans. Magn.*, vol. MAG-21, pp. 186–192, Mar. 1985.

[10] B. M. Oliver, "Directional electromagnetic couplers," *Proc. IRE*, vol. 42, pp. 1686–1692, Nov. 1954.

[11] J. R. Klauder, A. C. Price, S. Darlington, and W. J. Albersheim, "The theory and design of chirp radars," *Bell Syst. Tech. J.*, vol. 39, pp. 745–808, July 1960.

[12] R. S. Withers and P. V. Wright, "Superconductive tapped delay lines for low-insertion-loss wideband analog signal-processing filters," in *Proc. 37th Ann. Symp. Frequency Control* (Philadelphia), 1983, pp. 81–86.

[13] A. C. Anderson, R. S. Withers, S. A. Reible, and R. W. Ralston, "Substrates for superconductive analog signal processing devices," *IEEE Trans. Magn.*, vol. MAG-19, pp. 485–489, 1983.

Mark S. DiIorio was born in Winchester, MA, on May 16, 1958. He received the A.B. degree from Dartmouth College in 1980 and the Ph.D. degree in applied physics from Stanford University in 1985.

In 1985 he joined the Analog Device Technology Group of M.I.T. Lincoln Laboratory, where he has developed wide-band superconductive tapped delay lines and demonstrated their utility in real-time multigigahertz-bandwidth spectrum analysis. More recently, he has evaluated the RF characteristics of superconducting YBaCuO thin films. He is currently with Biomagnetic Technology, Inc., San Digeo, CA, where his work concerns the production of SQUID's of the new high-transition-temperature superconductors.

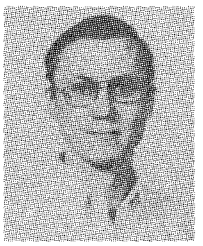

Richard S. Withers (S'78–M'78) was born in Davidson, NC, in 1953. He received the S.B. and S.M. degrees in electrical engineering from M.I.T. in 1976, with a thesis on surface spectrometry done at the Naval Surface Weapons Center. A National Science Foundation Graduate Fellow, he received the Sc.D. degree, also in electrical engineering, from M.I.T. in 1978, with a thesis in electrohydrodynamics.

Since 1978 he has worked in the Analog Device Technology Group at the M.I.T. Lincoln Laboratory, first as a staff member and at present as the Associate Group Leader, where he has been engaged in the development of analog signal processing devices such as nonvolatile analog semiconductor memory, charge-coupled devices, focal-plane image processors, acoustoelectric correlators, and, most recently, miniature superconductive tapped delay lines and correlators.

Alfredo C. Anderson was born in Rio de Janiero, Brazil, on December 8th, 1942. He received the B.S. and M.S. degrees in electrical engineering from the Instituto Technologico de Aeronautica (ITA), Brazil, in 1965 and 1968, respectively, and the Ph.D. degree from the University of California, Berkeley, in 1979. His dissertation was a study of the electronic properties of amorphous germanium.

From 1967 to 1973 he was associated with the Electrical Engineering Department of ITA, first as Junior Professor and later as Assistant Professor, where he taught courses on the physics of semiconductors and integrated circuits. In 1975 he was lecturer in the Electrical Engineering Department at the University of California, Berkeley. He joined M.I.T. Lincoln Laboratory in 1979 as a staff member in the Analog Device Technology Group, where he is contributing to the development of new technologies for the fabrication of superconductive, acousto-optic, and acoustoelectric devices.